Original Article

http://dx.doi.org/10.3349/ymj.2013.54.1.123
pISSN: 0513-5796, eISSN: 1976-2437

Yonsei Med J 54(1):123-130, 2013

YMJ

Correlations of Dynamic Contrast-Enhanced Magnetic Resonance Imaging with Morphologic, Angiogenic, and Molecular Prognostic Factors in Rectal Cancer

Hye-Suk Hong,[1] Se Hoon Kim,[2] Hae-Jeong Park,[3] Mi-Suk Park,[3] Ki Whang Kim,[3] Won Ho Kim,[4] Nam Kyu Kim,[5] Jae Mun Lee,[6] and Hyeon Je Cho[7]

[1]Department of Medicine, Graduate School, Yonsei University, Seoul; Departments of [2]Pathology, [3]Radiology, [4]Internal Medicine, and [5]Surgery, Severance Hospital, Yonsei University College of Medicine, Seoul; [6]Department of Radiology, Yeouido St. Mary's Hospital, The Catholic University of Korea College of Medicine, Seoul; [7]Department of Radiology, Seoul Veterans Hospital, Seoul, Korea.

Received: February 8, 2012
Revised: March 16, 2012
Accepted: April 4, 2012
Corresponding author: Dr. Ki Whang Kim, Department of Radiology, Research Institute of Radiological Science, Severance Hospital, Yonsei University College of Medicine, 50 Yonsei-ro, Seodaemun-gu, Seoul 120-752, Korea.
Tel: 82-2-2228-7400, Fax: 82-2-393-3035
E-mail: kwkimyd@yuhs.ac

*This study was presented at the 67th Korean Congress of Radiology 2011, Seoul, Republic of Korea and at the 97th Scientific Assembly and Annual Meeting of Radiological Society of North America 2011, Chicago, IL, USA.

· The authors have no financial conflicts of interest.

Purpose: To investigate the correlations between parameters of dynamic contrast-enhanced magnetic resonance imaging (DCE-MRI) and prognostic factors in rectal cancer. **Materials and Methods:** We studied 29 patients with rectal cancer who underwent gadolinium contrast-enhanced, T1-weighted DCE-MRI with a three Tesla scanner prior to surgery. Signal intensity on DCE-MRI was independently measured by two observers to examine reproducibility. A time-signal intensity curve was generated, from which four semiquantitative parameters were calculated: steepest slope (SLP), time to peak (Tp), relative enhancement during a rapid rise (Erise), and maximal enhancement (Emax). Morphologic prognostic factors including T stage, N stage, and histologic grade were identified. Tumor angiogenesis was evaluated in terms of microvessel count (MVC) and microvessel area (MVA) by morphometric study. As molecular factors, the mutation status of the K-ras oncogene and microsatellite instability were assessed. DCE-MRI parameters were correlated with each prognostic factor using bivariate correlation analysis. A p-value of <0.05 was considered significant. **Results:** Erise was significantly correlated with N stage (r=-0.387 and -0.393, respectively, for two independent data), and Tp was significantly correlated with histologic grade (r=0.466 and 0.489, respectively). MVA was significantly correlated with SLP (r=-0.532 and -0.535, respectively) and Erise (r=-0.511 and -0.446, respectively). MVC was significantly correlated with Emax (r=-0.435 and -0.386, respectively). No significant correlations were found between DCE-MRI parameters and T stage, K-ras mutation, or microsatellite instability. **Conclusion:** DCE-MRI may provide useful prognostic information in terms of histologic differentiation and angiogenesis in rectal cancer.

Key Words: Colorectal neoplasms, prognosis, diagnostic imaging, magnetic resonance imaging

INTRODUCTION

The prognosis of newly diagnosed colorectal cancer (CRC) depends on various

clinical, laboratory, and histopathologic factors. Tumor extent, lymph node status, histologic tumor grade, and lymphatic and venous invasion are established prognostic factors, and they are still the most reliable. Other recently investigated factors are related to biologic and molecular alterations in tumors, including tumor angiogenesis, excretion of angiogenic cytokines, oncogene expression, and genomic alteration.[1] For the evaluation of angiogenesis in both normal and tumor tissues, measurement of microvessel density (MVD) by means of immunohistochemical study is the most widely used method.[2] Many investigations have found MVD to be a prognostic indicator of CRC.[2-5] Several oncogenes and tumor suppressor genes are commonly altered in CRC, and mutations in K-ras gene are particularly significant.[6] Complex genomic alterations are implicated in the tumorigenesis of gastrointestinal tract, and approximately 15% of CRCs have microsatellite instability (MSI).[7]

Dynamic contrast-enhanced magnetic resonance imaging (DCE-MRI) can be used to measure functional vascular changes such as alterations in blood volume and vascular permeability in tumors as well as in normal tissues. Quantitative or semiquantitative methods are used to analyze DCE-MRI data. It is well established that parameters obtained with DCE-MRI are significantly correlated with the degree of angiogenesis in various malignancies.[8]

Although several studies[9,10] have assessed tumor angiogenesis using DCE-MRI and explored correlations with some parameters of clinical outcome in CRC, no studies have been published correlating DCE-MRI with various prognostic indicators in rectal cancers. Therefore, the purpose of this study was to investigate the correlations between semiquantitative parameters obtained with DCE-MRI and morphologic, angiogenic, and molecular prognostic factors in rectal cancers.

MATERIALS AND METHODS

Patients

We analyzed data from 43 consecutive patients (30 men and 13 women; age range, 35-80 years) with clinically suspected rectal cancer who underwent rectal MRI as part of their initial workup between October 2007 and March 2008. DCE-MRI was performed as an incorporated sequence of MRI evaluation. Of 43 patients, 31 were diagnosed as resectable lesions on MRI and subsequently underwent curative surgery. Twelve patients were considered unresectable and underwent adjuvant chemoradiation therapy (CRT) before surgery. Twelve patients were excluded from the study due to the potential of CRT to alter the stage of the disease. We also excluded 2 of 31 patients with resectable lesions not visualized by DCE-MRI. Therefore, our final study population was composed of 29 patients (20 men and nine women; age range, 31-76 years) who underwent curative resection of rectal cancer. We identified morphologic prognostic factors including T stage, N stage, and histologic tumor grade based on histopathologic data. Medical records were retrospectively reviewed to determine K-ras mutation status and the presence of MSI. The study was approved by the institutional review board of our hospital. Informed consent was not required for this retrospective collection of patient information.

DCE-MRI study

DCE-MRI was obtained using a three Tesla MR Unit (Magnetom Tim Trio; Siemens Medical Solutions, Erlangen, Germany), and a phased-array multi-coil was applied. For dynamic scanning, one experienced radiologist selected a single axial slice that contained the largest tumor area referring to unenhanced MR images. In all subjects, we obtained gadolinium contrast (Gd-DTPA, Dotarem®; Guerbet, Nice, France)-enhanced T1-weighted dynamic imaging using a turbo fast low angle shot sequence with the following parameters: repetition time/echo time, 500/1.34 msec; flip angle, 8°; section thickness, 5 mm; number of total images, 200; acquisition time per slice, 0.36 sec; total scan time, 72 sec; field of view, 330 mm; and matrix, 256×125. Scanning was started at the intravenous administration of contrast agent (0.2 mL/kg of body weight) at a rate of 3 mL/s via the antecubital vein followed by a 20 mL saline flush using an automatic power injector (Spectris; Medrad, Pittsburgh, PA, USA).

On DCE-MRI series in each patient, a region of interest (ROI) was drawn freely within the tumor to encompass the largest area of enhancement. The ROIs covered areas between 1.3 and 8.5 cm^2. ROI measurements were independently performed by two radiologists, generating two sets of data for each patient (Fig. 1). A time-signal intensity curve (TIC) was automatically plotted using commercially available software (Syngo; Siemens Medical Solutions, Erlangen, Germany). An in-house mathematical program calculated four parameters from each curve: 1) the steepest slope (SLP) between two time points in a curve; 2) time to peak

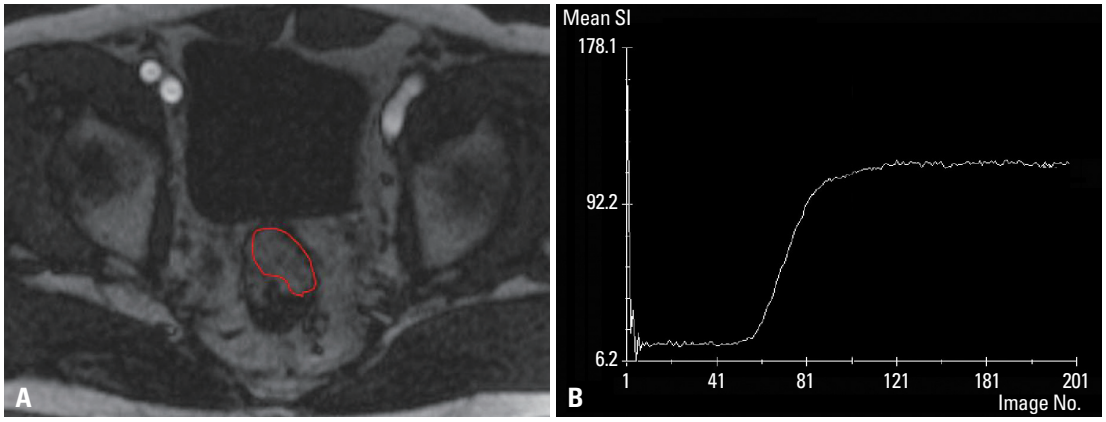

Fig. 1. Measurement of DCE-MRI. (A) On DCE-MRI, a ROI was freely drawn within the tumor to encompass the largest area of enhancement. (B) A time-signal intensity curve was generated at a workstation using commercially available software. DCE-MRI, dynamic contrast-enhanced magnetic resonance imaging; ROI, region of interest.

enhancement (Tp) in a curve, defined as the post-injection time to reach maximum signal intensity; 3) relative enhancement during a rapid rise (Erise), defined as SIrise-SIbase, in which SIrise indicates signal intensity during the rise, and SIbase is the mean signal intensity during the initial five time points; and 4) maximum relative enhancement (Emax) in a TIC, defined as SImax-SIbase, where SImax indicates the highest signal intensity in a curve. The parameters of TIC are schematically displayed in Fig. 2.

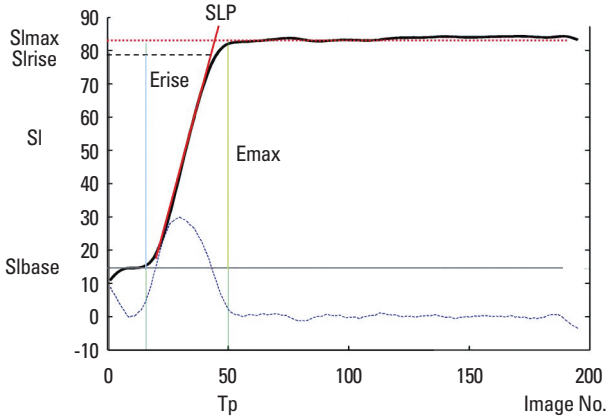

Fig. 2. Semiquantitative parameters of DCE-MRI in time-signal intensity curve. SLP is the steepest slope between two time points. Tp is time to peak enhancement. Relative enhancement during a rapid rise (Erise)=signal intensity during the rise (SIrise)-the mean signal intensity value during the initial five time points (SIbase). The maximum relative enhancement (Emax)=the highest signal intensity value in a curve (SImax)-SIbase. SI, signal intensity; Tp, time to peak; SLP, steepest slope; DCE-MRI, dynamic contrast-enhanced magnetic resonance imaging.

Morphometric analysis of microvessel density

With surgically-obtained paraffin-embedded tissue blocks, we selected a representative section containing tumoral and peritumoral tissues and prepared a four-μm-thick unstained slide for each patient. We performed immunohistochemistry with a Ventana BenchMark XT autostainer (Ventana Medical System Inc., Tucson, AZ, USA) according to the manufacturer's protocol using a CD31-related antigen-specific mouse monoclonal antibody (1 : 20 dilution; Dako, Carpinteria, CA, USA). An experienced pathologist selected four "hot spots" of greatest vascularization per low-power field (40×). High-power field (200×) images of the hot spots were digitally photographed by a microscope (DP72; Olympus, Tokyo, Japan) and stored as JPEG files (1550×1070 pixels, 16.7 million colors, 24-bit). Any brown-stained endothelial cells or endothelial cell cluster were considered a single, countable microvessel. Each microvessel was identified and outlined using commercialized software (Image-Pro Plus version 4.51; Media Cybernetics Inc., Silver Spring, MD, USA) (Fig. 3). The total number and area of microvessels were determined for each hot spot. We then calculated the mean total microvessel count (MVC) and mean total microvessel area (MVA) for each patient by averaging the values of four hot spots.

Mutation of K-ras oncogene

Genomic DNA was extracted from two or three four-μm-thick de-paraffinized tissue slides, containing representative portions of tumor tissue. DNA extraction was performed using the QIAamp DNA Tissue kit (Qiagen, Hilden, Germany), and 50 ng of DNA were amplified in a 20 μL reaction solution (10 μL of 2× concentrated HotStarTaq Master Mix; Qiagen, Hilden, Germany), including polymerase chain reaction (PCR) buffer with 3 mM magnesium chloride ($MgCl_2$), 400 μM deoxynucleotide triphosphates, and 0.3 μM each of primer pair (codon 12, 13, F: 5'-CGTCTG CAGTCAACTGGAAT, R: 5'-GAGAATGGTCCTGCAC CAGTAA). PCR products were 2% gel-purified with a

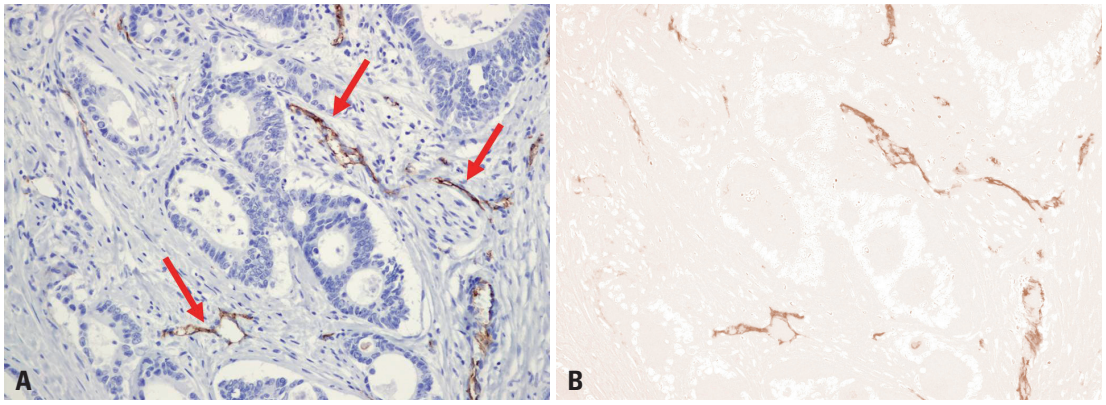

Fig. 3. Morphometric study of microvessels. Microvessels were immunostained using a CD31-related antigen-specific mouse monoclonal antiboy. (A) A photomicrograph (200×) of a hot spot in a representative tumor section shows immunostained microvessels (arrows) in brown. (B) Microvessels are highlighted by a color threshold setting to distinguish the objects of positive staining from the counterstained background tissue.

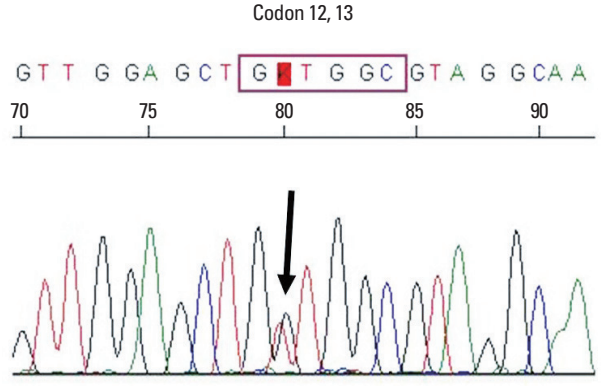

Fig. 4. DNA sequencing analysis of the K-ras gene. PCR products encompassing codons 12 and 13 of exon 2 were analyzed to confirm mutations. An overlap (arrow) of black G- and red T peaks at codon 12 is shown, representing a substitution of valine for glycine with G to T transversion. PCR, polymerase chain reaction.

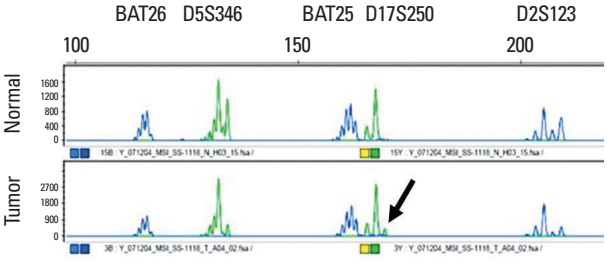

Fig. 5. A plot of electrophoregram analysis of microsatellite instability. The data of normal control (upper row) and tumor tissue (lower row) are displayed as base-pair size displayed on the x-axis against peak signal intensity in relative fluorescent units on the y-axis. A single, small peak (arrow) is additionally seen in tumor only with D17S250 marker, representing low-frequency of microsatellite instability (MSI-low).

QIAamp Gel Extraction Kit (Qiagen). DNA templates were processed for the sequencing reaction using the Big Dye Terminator Kit, version 3.1 (Applied Biosystems, Foster City, CA, USA) with both forward and reverse sequence-specific primers. The 10 μL sequencing reaction solution contained 20 ng of purified PCR products, 1 μL of Big Dye Terminator, and 0.1 μM the same PCR primers as listed above. Sequence data were generated with the ABI Prism 3100 DNA Analyzer (Applied Biosystems, Foster City, CA, USA) and analyzed by Sequencing Analysis 5.1.1. software (Applied Biosystems, Foster City, CA, USA) to compare variations (Fig. 4).

Assessment of MSI

DNA was extracted from all matched normal and tumor tissues for PCR amplification. A set of microsatellite markers consisting of two mononucleotide repeat markers (BAT25 and BAT26) and three dinucleotide repeat markers (D2S123, D5S346, and D17S250) was used to determine tumor MSI status. We amplified 50 ng of DNA in 20 μL of reaction solution containing 2 μL of 10× buffer (Roche, Mannheim, Germany), 1.7-2.5 mmol/L of $MgCl_2$, 0.3 μM each of primer pairs, 250 μM deoxynucleotide triphosphate, and 2.5 units of DNA polymerase (Roche, Mannheim, Germany). All PCR product samples were prepared for fragment separation on the ABI Prism 3100 Genetic Analyzer (Applied Biosystems, Foster City, CA, USA) using 0.7 μL of the amplified samples combined with 0.3 μL of the GeneScan 500 Size Standard (Applied Biosystems, Foster City, CA, USA) and 9 μL of HiDi formamide (Applied Biosystems, Foster City, CA, USA). Electrophoresis was initiated when the Genetic Analyzer oven temperature equilibrated to 60°C. Raw data were detected in real time as the fluorescence was converted to digital information and were processed at the workstation using the ABI Prism 3100 Data Collection software (Applied Biosystems, Foster City, CA, USA). Data were displayed as an electrophoregram: a plot of base-pair sizes displayed on the x-axis against peak sig-

Table 1. Distribution of the Values in Morphologic and Angiogenic Prognostic Factors

Morphologic factors			Angiogenic factors	
T	N	Histologic grade	MVC	MVA
T1 (1)	N0 (13)	Well differentiated (4)	5.0-20.5	0.3-31.2
T2 (6)	N1 (8)	Moderate (24)		
T3 (20)	N2 (8)	Poor (1)		
T4 (2)				

T, T stage; N, N stage; MVC, mean total microvessel count per field (40×); MVA, mean total microvessel area per field (40×).
Numbers in parenthesis are numbers of patients.

Table 2. Correlations of DCE-MRI with Morphologic and Angiogenic Factors

	Observer 1					Observer 2				
	T	N	Grade	MVC	MVA	T	N	Grade	MVC	MVA
SLP	0.003	-0.238	-0.089	-0.347	-0.532*	0.008	-0.266	0.007	-0.341	-0.511*
Tp	-0.041	0.025	0.466*	-0.256	0.150	-0.044	0.029	0.489*	-0.270	0.038
Erise	-0.059	-0.387*	-0.018	-0.357	-0.535*	-0.071	-0.393*	0.160	-0.367	-0.446*
Emax	-0.002	-0.213	0.162	-0.435*	-0.353	-0.039	-0.267	0.267	-0.386*	-0.354

T, T stage; N, N stage; Grade, histologic grade; MVC, mean total microvessel count per field (40×); MVA, mean total microvessel area per field (40×); SLP, steepest slope; Tp, time to peak enhancement; Erise, relative enhancement during a rapid rise; Emax, relative maximum enhancement; DCE-MRI, dynamic contrast-enhanced magnetic resonance imaging.
Data are correlation coefficients (rho, r) obtained by bivariate Spearman correlation analysis.
*Statistically significant (p<0.05) for both observers.

nal intensity (peak height) in relative fluorescent units on the y-axis (Fig. 5).

Statistical analysis

Bivariate Spearman correlation analysis was performed to investigate the correlations between DCE-MRI parameters and prognostic factors. The correlation coefficient (rho, r) was calculated and considered to be statistically significant when the two-tailed p-value was less than 0.05. To test the reproducibility of DCE-MRI measurements independently obtained by two observers, intra-class correlation coefficient (ICC) values for the parameters of two DCE-MRI data sets were calculated with a 95% confidence interval (CI). Data processing and statistical analysis were performed using the SPSS 18.0 statistical program (SPSS Inc., Chicago, IL, USA).

RESULTS

SLP ranged 0.43-2.17 (mean±SD, 1.19±0.49) for observer 1 and 0.33-2.08 (1.14±0.48) for observer 2. Tp ranged 21.24-70.56 sec (47.50±19.12) and 20.52-70.56 sec (47.71±18.94) for the two observers, respectively. Erise ranged 22.22-94.21 (47.00±17.56) and 17.00-91.46 (45.49±18.41), respectively, and Emax was 22.90-99.43 (52.57±20.07) and 17.11-98.28 (50.25±22.02), respectively.

The distribution of each morphologic factor and the values of each angiogenic marker are provided in Table 1. In the analysis of the K-ras mutation, mutant type was found in 6 of the 29 patients. In the 6 tumors, mutated K-ras was found in codons 12 and 13 located in exon 2. Four showed mutations at codon 12; a substitution of valine for glycine involving a base position (bp) 35 guanine-to-thymidine change (G to T transversion) in 2 and serine for glycine involving bp 34 guanine-to-adenine (G to A transition) in 2. The remaining two affected codon 13 with a substitution of aspartic acid for glycine, bp 38 G to A transition. Of the 29 patients, only one showed a low-frequency of microsatellite alteration (MSI-low), in which a single peak was observed only with D17S250 marker (Fig. 5). The remaining 28 showed microsatellite stable. Table 2 summarizes the correlations of DCE-MRI with morphologic and angiogenic prognostic factors. For both observers, Tp was positively correlated with histologic tumor grade (r=0.466, p=0.01; r=0.489, p=0.01; respectively), i.e. poorly differentiated tumors showed longer time to reach the peak enhancement compared with that of well differentiated lesions. Erise was negatively correlated with N stage for both observers (r= -0.387, p=0.04; r=-0.393, p=0.03; respectively). In the correlations between DCE-MRI and tumor angiogenesis, for both observers, MVA was significantly correlated with SLP (r= -0.532, p=0.003; r=-0.511, p=0.005; respectively) and Erise (r=-0.535, p=0.003; r=-0.446, p=0.015; respectively).

MVC was significantly correlated with Emax for both observers (r=-0.435, p=0.02; r=-0.386, p=0.04; respectively). None of the imaging parameters were significantly correlated with K-ras mutations or presence of MSI for either observer.

In the evaluation of inter-observer agreement for the independent sets of DCE-MRI parameters, ICC values for each parameter showed almost perfect level of agreement; 0.902 (0.802-0.953, 95% CI) for SLP, 0.902 (0.802-0.953, 95% CI) for Tp, 0.916 (0.829-0.960, 95% CI) for Erise, and 0.911 (0.819-0.957, 95% CI) for Emax.

DISCUSSION

The prognosis of newly diagnosed CRC predicts not only long-term clinical outcome, but also determines treatment strategy and patient selection for optimal therapy. The estimation of prognosis largely relies on the morphologic or anatomic extent of disease based on established staging classifications. The tumor node metastasis staging system remains the gold standard of prognostic factors in CRC.[1] However, heterogeneous outcomes and different responses to therapy among patients with histologically identical stages have prompted investigations into biologic and molecular tumor alterations as additional factors in prognosis. Previous research has shown that the degree of angiogenesis is related to tumor progression, lymph node and liver metastases, and survival in CRC.[2,3,11] K-ras mutations have been identified in 40-50% of CRCs; several reports have linked genotypic alterations of K-ras to stratification of prognosis.[6,12] Approximately 15% of CRCs exhibit MSI, which is characterized by the inactivation of a mismatch repair gene and is currently being investigated as one of the promising molecular markers of outcome. According to a meta-analysis by Popat, et al.,[7] CRC patients with MSI were found to have a significantly better prognosis compared to those with intact mismatch repair genes.

Quantification of tumor angiogenesis is typically assessed by counting microvessels in immunostained tissue sections. This technique is invasive and requires biopsy or surgery for tissue sampling. Other drawbacks are inherent inter-observer variability in selecting vascular hot spots, technical limitations such as sampling bias, and methodological discrepancies in the use of antibodies for immunostaining and counting vessels.[13] MVD count is a static structural assessment of the microvasculature that does not reflect functional status. DCE-MRI has shown high correlation with MVD[14-16] and is capable of depicting functional vascular changes such as alterations in blood volume and vascular permeability in many tumors.[8,17-19] Many studies have described the promising role of DCE-MRI in evaluating tumor angiogenesis in various human malignancies[16,20,21] including CRC.[9,10] Our study also showed significant correlations between parameters of DCE-MRI and tumor angiogenesis quantified by microvessel count and area in patients with rectal cancer.

Among the DCE-MRI parameters in our study, time to peak enhancement was significantly correlated with histologic tumor grade. A similar correlative study by Tuncbilek, et al.[10] found that histologic grade was significantly correlated with steepest slope and maximal enhancement of DCE-MRI, but not with time to peak, differing from our results. Semiquantitative parameters of DCE-MRI are obtained by interpreting changes in signal intensity as a function of time displayed by a curve, i.e., curvology. These parameters are indirectly related to changes in perfusion because there is no simple relation between changes in signal intensity and tissue concentration of contrast media. MRI signal intensity is dependent on many factors, including native tissue relaxation rates, contrast agent dose, injection rate, choice of imaging sequence and parameters, machine gain, and scaling factors.[22] Therefore, semiquantitative results are not readily applicable from one institution to another, because of different imaging equipment and protocol.[23,24] The advantage of semiquantitative analysis is that it is relatively simple in estimating with T1-weighted MRI, whereas quantitative analysis requires conversion of MRI signal intensities to contrast concentration by complex pharmacokinetic modeling.[10] Another advantage of semiquantitative parameters is their high reproducibility, as shown in our results as well as those in the literature.[23] Currently, DCE-MRI has been standardized with several quantitative parameters[25] and used as a noninvasive imaging biomarker to measure the properties of tumor microvasculature.

In our study, N stage showed a negative correlation with Erise. Tumors with more advanced N stages showed less enhancement during the interval of rapid rise in signal intensity, compared with those with earlier stages. We cannot exactly explain the mechanism of this negative correlation, however, the semiquantitative parameter "Erise" does not necessarily mean the quantity or total amount of perfusion. DCE-MRI parameters represent physiologic properties of

tumor microvasculature such as rapidity of blood flow or permeability *in vivo*. In our study, we defined Erise as an enhancement of a certain interval during the scan, consequently, it may not indicate the amount of perfusion. To our best knowledge, this is the first observation in evaluating correlations of DCE-MRI parameters with morphologic prognostic factors in primary adenocarcinoma of the rectum.

We found no significant correlations between DCE-MRI and molecular factors. It may be attributed to a small number of positive samples in the molecular data, which might have produced misleading result. Further studies with larger number of patietns would better be able to detect significant results.

Our study has several limitations. First, the study population was relatively small in number, resulting in suboptimal power to detect differences. As previously mentioned, a few positive data in molecular prognostic factors might have influenced statistical analysis. Second, DCE-MRI data were analyzed by a semiquantitative method that is indirect in representing tissue perfusion and is not standardized among institutions. Third, the total scan time of 72 seconds in our study was relatively short to include later wash-out phase of perfusion. After extravasation from the vascular space to the interstitial space, reflux of contrast agent back to the vascular space occurs over several minutes. In this regard, DCE-MRI parameters in our study were not explored according to the phases of perfusion. Finally, our study was performed by retrospective analysis of patient data. The patient population included heterogeneous subgroups of CRC stages. Although significant results were obtained between DCE-MRI, morphologic nodal status, and histologic tumor grade, a larger cohort study of patients with identical CRC stage is warranted to investigate the correlations between imaging parameters and molecular markers.

In conclusion, some parameters of DCE-MRI showed significant correlations with N stage, histologic tumor grade, and degree of tumor angiogenesis. Although the measurement was semiquantitative and thus indirectly represents tumor microvasculature, DCE-MRI may provide useful prognostic information in terms of histologic differentiation and angiogenesis in rectal cancer.

ACKNOWLEDGEMENTS

This work was supported by scholarship of the Graduate school, Yonsei University.

REFERENCES

1. Zlobec I, Lugli A. Prognostic and predictive factors in colorectal cancer. J Clin Pathol 2008;61:561-9.
2. Takahashi Y, Tucker SL, Kitadai Y, Koura AN, Bucana CD, Cleary KR, et al. Vessel counts and expression of vascular endothelial growth factor as prognostic factors in node-negative colon cancer. Arch Surg 1997;132:541-6.
3. Takebayashi Y, Aklyama S, Yamada K, Akiba S, Aikou T. Angiogenesis as an unfavorable prognostic factor in human colorectal carcinoma. Cancer 1996;78:226-31.
4. Saclarides TJ, Speziale NJ, Drab E, Szeluga DJ, Rubin DB. Tumor angiogenesis and rectal carcinoma. Dis Colon Rectum 1994;37:921-6.
5. Choi HJ, Hyun MS, Jung GJ, Kim SS, Hong SH. Tumor angiogenesis as a prognostic predictor in colorectal carcinoma with special reference to mode of metastasis and recurrence. Oncology 1998;55:575-81.
6. Benhattar J, Losi L, Chaubert P, Givel JC, Costa J. Prognostic significance of K-ras mutations in colorectal carcinoma. Gastroenterology 1993;104:1044-8.
7. Popat S, Hubner R, Houlston RS. Systematic review of microsatellite instability and colorectal cancer prognosis. J Clin Oncol 2005;23:609-18.
8. Hylton N. Dynamic contrast-enhanced magnetic resonance imaging as an imaging biomarker. J Clin Oncol 2006;24:3293-8.
9. George ML, Dzik-Jurasz AS, Padhani AR, Brown G, Tait DM, Eccles SA, et al. Non-invasive methods of assessing angiogenesis and their value in predicting response to treatment in colorectal cancer. Br J Surg 2001;88:1628-36.
10. Tuncbilek N, Karakas HM, Altaner S. Dynamic MRI in indirect estimation of microvessel density, histologic grade, and prognosis in colorectal adenocarcinomas. Abdom Imaging 2004;29:166-72.
11. Des Guetz G, Uzzan B, Nicolas P, Cucherat M, Morere JF, Benamouzig R, et al. Microvessel density and VEGF expression are prognostic factors in colorectal cancer. Meta-analysis of the literature. Br J Cancer 2006;94:1823-32.
12. Finkelstein SD, Sayegh R, Christensen S, Swalsky PA. Genotypic classification of colorectal adenocarcinoma. Biologic behavior correlates with K-ras-2 mutation type. Cancer 1993;71:3827-38.
13. Vermeulen PB, Gasparini G, Fox SB, Colpaert C, Marson LP, Gion M, et al. Second international consensus on the methodology and criteria of evaluation of angiogenesis quantification in solid human tumours. Eur J Cancer 2002;38:1564-79.
14. Buadu LD, Murakami J, Murayama S, Hashiguchi N, Sakai S, Masuda K, et al. Breast lesions: correlation of contrast medium enhancement patterns on MR images with histopathologic findings and tumor angiogenesis. Radiology 1996;200:639-49.
15. Hawighorst H, Knapstein PG, Knopp MV, Vaupel P, van Kaick G. Cervical carcinoma: standard and pharmacokinetic analysis of time-intensity curves for assessment of tumor angiogenesis and patient survival. MAGMA 1999;8:55-62.
16. Leach MO. Application of magnetic resonance imaging to angiogenesis in breast cancer. Breast Cancer Res 2001;3:22-7.
17. Miller JC, Pien HH, Sahani D, Sorensen AG, Thrall JH. Imaging angiogenesis: applications and potential for drug development. J Natl Cancer Inst 2005;97:172-87.
18. Rehman S, Jayson GC. Molecular imaging of antiangiogenic agents. Oncologist 2005;10:92-103.

19. Park HC, Shimizu S, Yonesaka A, Tsuchiya K, Ebina Y, Taguchi H, et al. High dose three-dimensional conformal boost using the real-time tumor tracking radiotherapy system in cervical cancer patients unable to receive intracavitary brachytherapy. Yonsei Med J 2010;51:93-9.
20. Hawighorst H, Knapstein PG, Weikel W, Knopp MV, Zuna I, Knof A, et al. Angiogenesis of uterine cervical carcinoma: characterization by pharmacokinetic magnetic resonance parameters and histological microvessel density with correlation to lymphatic involvement. Cancer Res 1997;57:4777-86.
21. Schlemmer HP, Merkle J, Grobholz R, Jaeger T, Michel MS, Werner A, et al. Can pre-operative contrast-enhanced dynamic MR imaging for prostate cancer predict microvessel density in prostatectomy specimens? Eur Radiol 2004;14:309-17.
22. Goh V, Padhani AR, Rasheed S. Functional imaging of colorectal cancer angiogenesis. Lancet Oncol 2007;8:245-55.
23. Galbraith SM, Lodge MA, Taylor NJ, Rustin GJ, Bentzen S, Stirling JJ, et al. Reproducibility of dynamic contrast-enhanced MRI in human muscle and tumours: comparison of quantitative and semi-quantitative analysis. NMR Biomed 2002;15:132-42.
24. Gu J, Khong PL, Wang S, Chan Q, Wu EX, Law W, et al. Dynamic contrast-enhanced MRI of primary rectal cancer: quantitative correlation with positron emission tomography/computed tomography. J Magn Reson Imaging 2011;33:340-7.
25. Tofts PS, Brix G, Buckley DL, Evelhoch JL, Henderson E, Knopp MV, et al. Estimating kinetic parameters from dynamic contrast-enhanced T(1)-weighted MRI of a diffusable tracer: standardized quantities and symbols. J Magn Reson Imaging 1999;10:223-32.